ADAPTIVE MULTI-BAND LORA-BASED SYSTEM FOR DATA TRANSMISSION IN CIVIL DEFENCE MONITORING AND ALERTING

Rodions Saltanovs[1], Alexey Shevchenko[2], Janis Usans[3]
[1]Riga Nordic University, Latvia; [2]SIA "RS DYNAMICS", Latvia; [3]SIA "Strive", Latvia
bk201@inbox.lv, alexey@cryptolab.net, janis@strive.lv

Abstract. This paper presents a physically implemented multi-band LoRa-based backup communication prototype for civil-defence telemetry and alerting built on a software-defined radio platform. The prototype operates on five bands (150 MHz, 430 MHz, 868 MHz, 1.2 GHz, and 2.4 GHz), supports rapid retuning, and includes a preliminary mesh-capable forwarding layer intended to reduce dependence on fixed gateway infrastructure. To enable fair cross-band comparison, the effective isotropic radiated power of all paths was equalized using calibrated attenuators. Baseline experiments on an approximately 6.07 km line-of-sight link under a common LoRa configuration show a clear frequency-dependent trend: 150/430 MHz provide the strongest received signal, highest SNR, and lowest packet error rate, while 2.4 GHz remains usable but more margin-limited. Representative application-layer throughput was approximately 2-5 kbps on a conservative single channel and 20-30 kbps when traffic was distributed across all five bands under favourable conditions. The main contribution of the paper is an experimentally grounded cross-band engineering comparison and system-integration reference rather than a complete mesh or anti-jamming validation. The results support the use of lower bands as robust backbone control links and higher bands as supplementary channels for burst capacity and diversity, while motivating broader non-line-of-sight, multi-hop, and interference-oriented validation in future work.

Keywords: LoRa, software-defined radio, multi-band communication, gateway-free networking, emergency telemetry, frequency diversity.

Introduction

Emergency warning and civil-defence systems require communication links that remain available when commercial infrastructure is degraded, overloaded, or untrusted. In such situations, a control centre must still be able to activate and supervise distributed sirens and field devices even during cellular outages or degraded backhaul. Reviews of public-safety and harsh-environment communication consistently identify resilience, autonomy, and technology diversity as key design requirements [1-3].

LoRa is attractive for this role because it combines long communication range, low power consumption, and robust chirp-spread-spectrum signalling [4; 5]. However, conventional LoRaWAN depends on gateway-centred star networking and has practical limits in throughput, scalability, duty-cycle usage, and coordinated downlink support [5-7]. These limits motivate direct peer-to-peer links, multi-hop forwarding, and alternative channel plans for resilient field communications [8-13].

The present work combines three ideas in one physically implemented prototype: multi-band LoRa operation across five widely separated RF channels, a gateway-independent point-to-point and preliminary mesh-capable networking model, and an IP-over-LoRa adaptation layer for command and telemetry traffic. The contribution is not a new LoRa physical layer or a new routing theorem. Instead, the paper provides an experimentally grounded system design showing how frequency diversity, EIRP-equalized comparison, and a compact SDR implementation can support resilient civil-defence communications.

Beyond the specific civil-defence scenario, the study is also motivated by a broader rural-engineering problem: sparse territories often depend on long-distance, low-rate communication links where infrastructure redundancy is limited, and service recovery may be slow. A multi-band LoRa prototype is therefore relevant not only as a public-warning backup, but also as a reference architecture for distributed monitoring and control when commercial connectivity is unavailable or unreliable.

The specific contributions of this study are as follows.

1. The design and physical implementation of a five-band LoRa-capable SDR node for infrastructure-independent civil-defence telemetry and alerting.
2. A calibrated cross-band comparison methodology based on approximately equalized EIRP across 150 MHz, 430 MHz, 868 MHz, 1.2 GHz, and 2.4 GHz.
3. An experimental baseline dataset obtained on the same 6.07 km line-of-sight path using a common LoRa configuration and common packet structure.

4. An engineering interpretation of role separation between lower-frequency backbone control channels and higher-frequency auxiliary channels for burst capacity and diversity.

The paper therefore addresses a narrower but practically important question: how does one physically implemented multi-band LoRa-capable SDR platform behave across widely separated frequency bands when the comparison is performed under equalized radiated power and common packet settings on the same path.

Related work

Resilient emergency communication research emphasizes heterogeneous and layered architectures rather than dependence on a single band or infrastructure domain [1-3]. Multi-channel and cognitive-radio studies further show that distributing traffic across several frequencies can improve robustness under interference and partial-band denial [14; 15].

For LoRa specifically, reviews and experimental studies show that the technology is well suited to long-range low-rate telemetry, but that conventional LoRaWAN has architectural and scalability limits in demanding scenarios [4-8]. A substantial body of work has therefore explored LoRa mesh and multi-hop systems, including peer-to-peer LoRa meshes, synchronized multi-hop networks, and application-specific forwarding schemes for monitoring and emergency messaging [8-13; 16; 17].

Compared with previous studies, the present prototype emphasizes combined frequency diversity and gateway-free networking for civil-defence control links. The work also adds a practical cross-band methodology by equalizing radiated power across all tested frequencies before comparing RSSI, SNR, PER, PDR, and RTT on the same 6 km path.

Earlier LoRa mesh and multi-hop studies optimize a single operating band, a specific routing approach, or a narrow application scenario. In contrast, the present work addresses a different engineering question: the comparative cross-band behavior of one gateway-free, SDR-based node architecture under approximately equalized EIRP and a common packet configuration on the same path. The contribution of the present article is therefore primarily integrative and experimental. It does not replace detailed mesh-protocol research but complements it by providing a practical multi-band baseline relevant to resilient emergency telemetry and sparse-territory monitoring.

System architecture and methods

Each node is built around a Xilinx Zynq-7020 SoC and an AD9361-class SDR transceiver, with embedded Linux handling control logic and higher-layer networking. The RF front-end provides five band-specific paths at 150 MHz, 430 MHz, 868 MHz, 1.2 GHz, and 2.4 GHz. Each path includes transmit/receive switching, filtering, power amplification, and calibrated attenuation. A GPS-disciplined oscillator provides a 10 MHz reference and a 1 PPS signal for coordinated timing, optional TDMA-like scheduling, and synchronized band switching.

The platform supports three operating modes. In single-band mode a node remains on a selected primary channel. In adaptive switching mode the node monitors RSSI, SNR, packet errors, and noise floor and can retune to an alternate band when interference or fading degrades the active link. In multi-band aggregation mode traffic is distributed across several bands to increase burst throughput. Lower bands are intended for robust control links, while higher bands provide supplementary capacity when line-of-sight and spectrum conditions permit.

Above PHY, a lightweight adaptation layer transports bounded IPv6/UDP traffic over LoRa. The layer performs header compression, fragmentation and reassembly, and link-aware reliability using ARQ for critical traffic. A compact forwarding layer provides point-to-point operation and preliminary mesh-capable routing. Nodes are functionally identical; there is no fixed gateway, and any node can relay traffic or serve as an ingress/egress point when backhaul is available.

Routing is deliberately lightweight to match LoRa airtime constraints. Nodes periodically exchange compact beacons, maintain only minimal neighbour and next-hop state, and can use controlled flooding for high-priority broadcasts when route knowledge is incomplete. The current prototype assumes pre-shared credentials, applies AES-256 encryption at the network layer, and may add link-layer cryptographic protection for control traffic. A full security analysis, including key management and replay protection, is outside the scope of the present paper.

From a security perspective, the present prototype assumes pre-shared credentials and focuses on confidentiality and basic access control at the network layer. The main considered threats are unauthorized command injection, message interception, replay of previously observed control frames, and node impersonation. The current implementation addresses confidentiality of payload transport, but it does not yet provide a complete operational key-management framework, formal replay-protection analysis, secure bootstrapping, or resistance to physical node capture. These aspects are recognized as important for civil-defense deployment and remain a dedicated direction for future work.

To compare frequencies fairly, the effective isotropic radiated power of each path was equalized to approximately 100 mW using calibrated attenuators. This compensates for different antenna gains and RF-chain losses and prevents the lower bands from being artificially favoured by transmit-power bias. The selected bands were chosen to balance propagation and practicality: 150 and 430 MHz provide the largest range margin; 868 MHz offers compatibility with widely used LoRa deployments; 1.2 GHz adds specialized diversity; and 2.4 GHz serves as an opportunistic higher-capacity link.

The resulting architecture is intentionally asymmetric. Lower bands are treated as the preferred control and alarm channels because they preserve the largest fade margin and remain compatible with modest-gain omnidirectional antennas. Higher bands are kept in the design not because they outperform VHF/UHF on long links, but because they offer supplementary diversity, localized capacity, and operational flexibility when geometry or spectrum conditions favour them. This distinction between backbone and auxiliary roles is central to the interpretation of the measurements reported later.

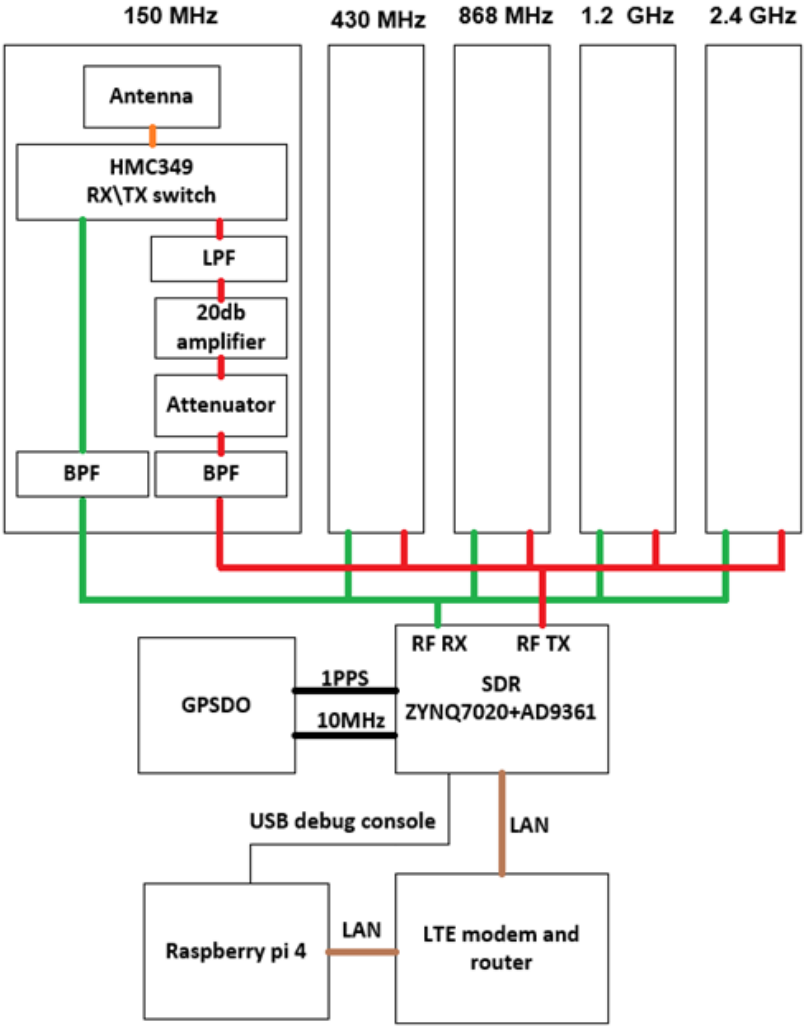

Fig. 1. **Simplified hardware structure of one multi-band SDR node and its external support equipment**

Experimental setup

Baseline experiments were performed on an approximately 6.07 km line-of-sight path measured by GPS. Two identical SDR nodes were placed at modest antenna heights and tested sequentially on each band under the same geometry and nominal RF configuration. One endpoint additionally used LTE for remote management, but all reported performance metrics were measured over the radio link itself.

Before field measurements, each RF path was calibrated so that the effective isotropic radiated power was approximately 100 mW on every band. This equalization compensates for differences in antenna gain, amplifier gain, and front-end losses, allowing the measured RSSI/SNR/PER/PDR trends to be interpreted primarily as propagation and margin effects rather than as transmit-power bias. The selected bands span VHF to 2.4 GHz in order to contrast long-range robustness with opportunistic higher-frequency capacity.

The common LoRa PHY configuration for the baseline comparison was spreading factor SF = 9, bandwidth BW = 125 kHz, coding rate CR = 4/5, payload = 16 bytes, and preamble = 8 symbols. Packet delivery statistics were computed over N = 1000 trials per band. The recorded metrics were RSSI, SNR, packet error rate (PER), packet delivery ratio (PDR), and round-trip time (RTT). These values should be interpreted as baseline single-link measurements rather than full mesh-level performance.

Table 1

Measured 6 km line-of-sight link performance under equalized EIRP and a common LoRa configuration

Band	RSSI, dBm	SNR, dB	PER, %	PDR, %	RTT, ms
150 MHz	-72	26	0.1	99.9	240
430 MHz	-78	24	0.2	99.8	250
868 MHz	-83	22	0.8	99.2	285
1.2 GHz	-86	20	1.4	98.6	310
2.4 GHz	-94	10	4.5	95.5	390

Each band was evaluated using the same packet structure and the same nominal PHY configuration so that the observed differences would primarily reflect propagation and RF-chain behaviour rather than protocol changes. Test packets were exchanged in repeated ping-style cycles, and the resulting RSSI, SNR, PER, PDR, and RTT values were aggregated over the full set of trials. This produces a compact but comparable baseline for all five channels and provides the quantitative reference used in the later deployment discussion.

Statistical and analytical treatment

For each band, packet delivery statistics were computed over N = 1000 packet trials. Packet delivery ratio was calculated as

$$PDR = \frac{N_{success}}{N} \times 100\% \tag{1}$$

and packet error rate as

$$PER = \frac{N_{error}}{N} \times 100\% = 100\% - PDR \tag{2}$$

Because packet delivery is a binary outcome (successful/unsuccessful), 95% confidence intervals for PDR were estimated using the Wilson score interval. This provides a more informative statistical summary than reporting only aggregate percentages.

To relate the measured cross-band trend to a simple analytical propagation reference, the observed degradation was also compared with the relative free-space path-loss scaling expected at constant distance,

$$\Delta FSPL\_i = 20\lg\left(\frac{f_i}{f_{ref}}\right) \tag{3}$$

where f_{ref} = 150 MHz – was used as the reference frequency for relative comparison.

This comparison is not intended to replace a full site-specific propagation model, but to show whether the measured monotonic cross-band trend is broadly consistent with frequency-dependent propagation expectations.

Table 2

Statistical summary of packet delivery over $N = 1000$ trials per band

Band	Successful packets/1000	PDR, %	95% CI for PDR, %	PER, %
150 MHz	999	99.9	99.44-99.98	0.1
430 MHz	998	99.8	99.27-99.95	0.2
868 MHz	992	99.2	98.43-99.59	0.8
1.2 GHz	986	98.6	97.66-99.16	1.4
2.4 GHz	955	95.5	94.03-96.62	4.5

Note: 95% confidence intervals were estimated using the Wilson score interval for binomial outcomes

Results and discussion

The measured results show a consistent monotonic deterioration of link quality with increasing carrier frequency (Fig. 2). As shown in Fig. 2(a) and Fig. 2(b), RSSI and SNR decrease progressively from 150 MHz to 2.4 GHz under the same 6.07 km line-of-sight geometry, approximately equalized EIRP, and common LoRa PHY settings. This reduction in link margin is directly reflected in latency and delivery performance: RTT increases with carrier frequency, as shown in Fig. 2(c), while the corresponding packet-delivery trend, together with the 95% confidence intervals, is summarized in Fig. 2(d). Under the tested geometry, all five bands remained operational; however, the lower bands are clearly the strongest candidates for backbone control links, whereas the higher bands are better treated as supplementary channels with lower margin.

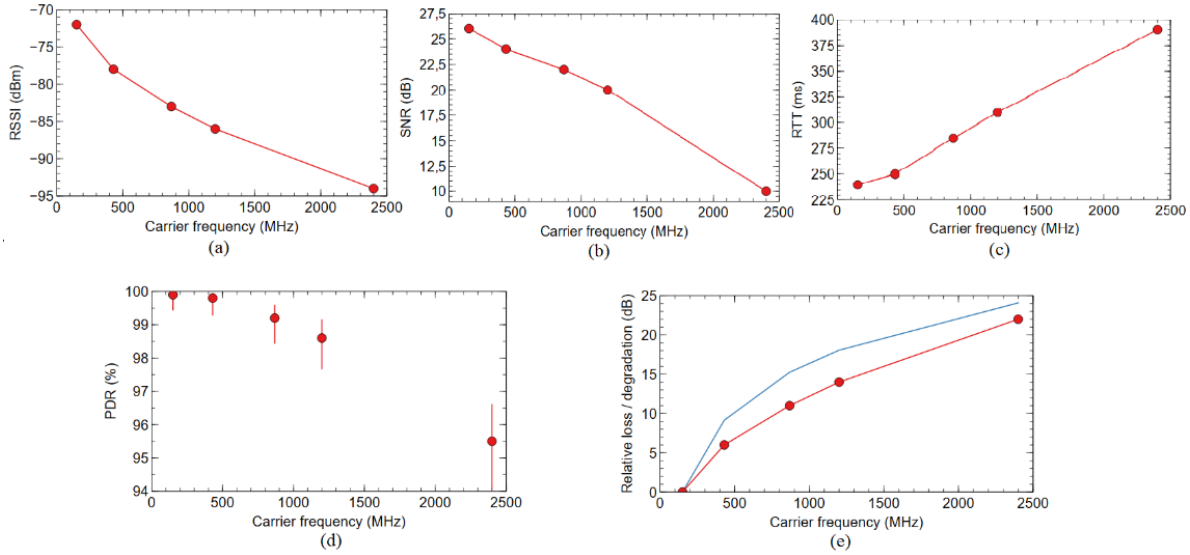

Fig. 2. **Cross-band baseline performance of the proposed multi-band LoRa SDR system on the 6.07 km line-of-sight link under approximately equalized EIRP and a common LoRa configuration:** a – measured RSSI versus carrier frequency; b – measured SNR versus carrier frequency; c – measured RTT versus carrier frequency; d – measured PDR with 95% confidence intervals over $N = 1000$ trials per band; e – measured RSSI degradation relative to 150 MHz compared with the relative free-space path-loss reference

To relate the measured trend to a simple analytical reference, the cross-band RSSI degradation was compared with the relative free-space path-loss increase expected from frequency scaling at constant distance. Relative to 150 MHz, the measured RSSI decreased by approximately 6 dB at 430 MHz, 11 dB at 868 MHz, 14 dB at 1.2 GHz, and 22 dB at 2.4 GHz, while the corresponding free-space reference increases are approximately 9.1 dB, 15.2 dB, 18.1 dB, and 24.1 dB. Although exact agreement is not expected because of antenna behaviour, RF front-end characteristics, calibration residuals, and site-

specific conditions, the measured monotonic trend is broadly consistent with frequency-dependent propagation expectations.

Application-layer throughput followed the same pattern. In the baseline point-to-point tests a single conservative LoRa channel provided approximately 2-5 kbps, while parallel use of the five bands yielded about 20-30 kbps aggregate throughput under favourable conditions. These values are sufficient for command messages, acknowledgments, compact telemetry, and periodic status reporting. They do not imply that 128 kbps sustained throughput was demonstrated; rather, they show that multi-band aggregation can provide useful burst capacity and redundancy for low-rate emergency workloads.

From an application perspective, these data rates should be interpreted against the actual message profile of a civil-defence backup link. Siren activation commands, acknowledgments, heartbeat packets, compact status telegrams, and sensor summaries impose very small payload volumes but require high delivery confidence and predictable access. In that context, even a few kilobits per second can be operationally sufficient when the channel is managed conservatively. The relevance of multi-band aggregation is therefore not primarily high-volume transport, but the ability to absorb retransmissions, brief reporting bursts, and parallel low-rate services without overloading the lowest-frequency control path.

Interference behaviour was assessed in this study primarily through simulation informed by the measured baseline SNR values rather than through dedicated field interference experiments. The purpose of this analysis is not to claim field-validated anti-jamming performance, but to illustrate how multi-band frequency agility may help preserve low-rate service when one channel becomes degraded. Under these assumptions, the simulation indicates that broadband noise degrades LoRa links gradually, whereas narrowband interference can more rapidly disrupt margin-limited channels. These observations should therefore be interpreted as simulation-supported engineering evidence only.

Although the prototype includes a preliminary mesh-capable forwarding layer, the quantitative validation reported in this paper is primarily single-link and point-to-point. Preliminary relay observations suggest that a multi-hop deployment may extend coverage by replacing one marginal long hop with multiple shorter hops, but the present manuscript does not claim full mesh-network validation. A dedicated multi-hop campaign with controlled topology, hop-count variation, route-failure testing, and end-to-end delay analysis remains for future work.

Observability is an additional practical consideration for a multi-band emergency network. In the present work, this aspect is treated separately and only at a theoretical level: multi-band operation can improve resilience, but may also increase spectral observability if transmissions are regular and predictable. A compact theoretical discussion is therefore included in Section 6, while dedicated receiver-side validation remains for future work.

Taken together, the measurements and simulation-informed observations suggest a clear operating policy rather than a single universally best frequency. The engineering value of the prototype lies in its ability to assign different roles to different bands: robust long-range supervision at lower frequencies, supplementary throughput and local relay opportunities at higher frequencies, and fallback options when one portion of the spectrum becomes unreliable. For emergency telemetry, this role-based interpretation is more useful than a simple ranking of channels by raw link margin alone.

This role separation also explains why the system was designed around a multi-band SDR rather than around a single optimized transceiver path. A single low-frequency channel would maximize range but would provide limited flexibility under congestion, local interference, or changing mission geometry. Conversely, a high-frequency-only design would simplify hardware in some respects but would sacrifice the margin needed for dependable wide-area alerting. The prototype therefore treats frequency diversity as a systems-engineering mechanism: different channels are not interchangeable, but each contributes a distinct operating function within the overall backup network.

Theoretical considerations on multi-band network detectability

An additional question relevant to the proposed architecture and to future drone-assisted relay development is how easily the presence of the network can be detected by an external spectrum-monitoring receiver. Because the system operates across several preselected bands and may use synchronized or repeated transmissions for control, telemetry, or failover, it can create observable

signatures in both frequency and time. While multi-band operation improves communication resilience, it can also increase the number of spectral windows in which activity may be observed.

At the simplest level, detection can be based on received energy. For a monitored band i, a detector may evaluate

$$T_i = \frac{1}{N_i} \sum_{n=1}^{N_i} |r_i[n]|^2 , \quad (4)$$

where $r_i[n]$ – received signal
N_i – number of observed samples.

If T_i exceeds a threshold, the observer declares that transmission is present. In a multi-band case, the observer may combine several such decisions, so the probability of detecting at least one burst increases with the number of monitored bands. Detection becomes even easier if the observer exploits prior knowledge of LoRa-like waveforms, repeated packet structures, or cross-band timing regularities.

At the same time, detectability is reduced when traffic is sparse, packet duty cycle is low, and activity is distributed across multiple bands rather than concentrated on one continuously active channel. The absence of a permanently active gateway may also reduce the likelihood of continuous observation at a fixed spectral position. Therefore, in the present architecture, detectability depends mainly on observation time, receiver sensitivity, prior knowledge of candidate bands and waveform family, and the degree of temporal coordination used by the network.

This section is intentionally theoretical and is included to frame an adjacent engineering question rather than to claim a validated detection model. A full receiver-side study would require dedicated monitoring experiments and ROC-based detector evaluation under realistic field conditions, including future comparisons between ground-only and drone-assisted relay configurations.

Deployment considerations

Antenna selection is a practical determinant of performance, especially at the higher bands. In the measured 6 km scenario, 150 and 430 MHz had sufficient margin that modest-gain antennas remain acceptable, which is advantageous for wide-area mesh coverage. At 2.4 GHz, by contrast, directional gain is important for maintaining a reliable link. A realistic deployment strategy is therefore hybrid: lower bands use omnidirectional or modest-gain antennas for resilient coverage, while upper bands use directional antennas where geometry is known and burst capacity is desired.

The networking strategy should follow the same asymmetry. Lower bands are well suited to a continuously available control plane because they retain the best link margin and tolerate modest-gain omnidirectional antennas. Higher bands are more naturally assigned to auxiliary data bursts, local relay segments, or point-to-point links with known geometry. This division also helps manage power draw, since only the currently active RF chain must remain fully energized while secondary receivers can be duty-cycled until needed.

Multi-band hardware also affects power and observability. Power consumption can be managed by activating only the current transmit chain and duty-cycling secondary receivers while maintaining one always-listening control band. From an observability standpoint, the use of multiple preselected bands improves communication resilience but may also create detectable activity across more spectrum. In this paper, that issue is addressed only at a theoretical level in Section 6 and is not part of the core experimental validation.

In rural and semi-rural deployments, this layered operating policy has practical management advantages. A permanent low-band supervisory channel can remain available for health monitoring, alarm dispatch, and minimal telemetry, while higher bands are activated only when larger status exchanges, local relay tasks, or short high-quality paths are needed. Such a strategy reduces average energy consumption, limits unnecessary spectrum occupancy, and preserves the most robust channels for the traffic classes that are least tolerant to outage. It also aligns well with staged deployment, where a basic control plane may be commissioned first and auxiliary capacity, including possible drone-assisted relay segments, may be added later as operational needs grow.

Limitations and future work

The current validation is intentionally bounded. The experimental core of the paper is a controlled point-to-point comparison across five bands on a single 6 km line-of-sight path. This makes the frequency-dependent trend clear, but it does not yet quantify performance under dense vegetation, urban obstruction, non-line-of-sight terrain, or severe multi-user congestion. Likewise, the mesh component is presently supported by preliminary relay observations rather than by a full multi-hop campaign with controlled topology and route-failure testing.

A further limitation is that the present manuscript reports mainly aggregated baseline metrics rather than full packet-level distributions for all measured quantities. The added statistical treatment therefore focuses on delivery-related metrics that can be rigorously summarized from the available trial counts. More complete packet-level characterization, broader terrain diversity, and controlled interference measurements would further strengthen the generality of the conclusions. For this reason, the present results should be interpreted as a calibrated engineering baseline rather than as a universal deployment model for all operating environments.

Future work should therefore focus on four areas: broader field trials across different terrains and interference environments; quantitative multi-hop evaluation including hop-count, route repair, and end-to-end throughput; hardware refinement toward lower-power, lower-cost, and more compact multi-band nodes; and evaluation of drone-assisted relay configurations for extending coverage and improving deployment flexibility. Additional work on spectrum sensing, coordinated hopping, and integration with emergency management software would also strengthen the path from research prototype to deployable backup communication system.

Even with these limitations, the present study is informative because it isolates one essential variable – carrier frequency within a common SDR/LoRa framework – and examines its practical consequences under equalized radiated power. The article should therefore be read as a baseline engineering reference: not a final operational validation, but a grounded comparison that can guide subsequent field trials, hardware refinement, and integration with emergency-management workflows.

Accordingly, the present paper occupies an intermediate position between a concept paper and a full operational field trial. It contributes a physically implemented prototype, a calibrated cross-band comparison methodology, and a first set of measured results that reveal how frequency diversity can be exploited in a realistic backup-communication architecture. That combination is useful even before the full mesh layer, broader terrain campaign, or longer endurance testing are completed, because it provides a grounded basis for deciding which bands should carry critical control traffic and which should remain auxiliary.

Conclusions

This paper presented a physically implemented multi-band LoRa-based SDR prototype for backup civil-defense telemetry and alerting and reported a calibrated cross-band comparison under approximately equalized EIRP on a 6.07 km line-of-sight path. The measurements confirm a clear frequency-dependent baseline trend: lower bands provide stronger received signal, higher SNR, and better reliability, while higher bands remain useful as auxiliary channels when additional diversity or burst capacity is required.

The principal contribution of the study is an experimentally grounded engineering reference for multi-band role allocation rather than a complete operational validation of mesh networking or anti-jamming performance. From this baseline, VHF/UHF should be preferred for robust long-range control links, whereas 868 MHz, 1.2 GHz, and especially 2.4 GHz are better treated as opportunistic supplementary channels depending on regulation, geometry, and interference conditions. Broader terrain trials, dedicated multi-hop measurements, receiver-side detectability studies, and controlled interference experiments are the next steps.

Author contributions

Rodions Saltanovs developed the study concept and designed the experimental framework. Alexey Shevchenko developed the software and performed data collection. Jānis Usānse assembled the

prototype hardware. All authors contributed to manuscript review and approved the final version of the manuscript.

Acknowledgments

This work was supported by European funding under project No. 2.2.1.3.i.0/2/24/A/CFLA/001, "Development of a Dual Communication Civil Alert Siren Control System," and project No. 5.1.1.2.i.0/2/24/A/CFLA/002, "Research and development of smart drone detector."

References

[1] Baldini G., Karanasios S., Allen D., Vergari F. Survey of Wireless Communication Technologies for Public Safety. IEEE Communications Surveys & Tutorials. Vol. 16, no. 2, 2014, pp. 619-641.
[2] Ali K. et al. Review and Implementation of Resilient Public Safety Networks: 5G, IoT, and Emerging Technologies. IEEE Network. Vol. 35, no. 2, 2021, pp. 18-25.
[3] Bouras C., Gkamas A., Katsampiris Salgado S. A. Long Range Based IoT Search and Rescue System. Computer Networks and Communications. Vol. 1, no. 1. 2022, pp. 2-16.
[4] Augustin A., Yi J., Clausen T., Townsley W. M. A Study of LoRa: Long Range & Low Power Networks for the Internet of Things. Sensors. Vol. 16, no. 9, 2016.
[5] Haxhibeqiri J., De Poorter E., Moerman I., Hoebeke J. A Survey of LoRaWAN for IoT: From Technology to Application. Sensors. Vol. 18, no. 11, 2018.
[6] Adelantado F. et al. Understanding the Limits of LoRaWAN. IEEE Communications Magazine. Vol. 55, no. 9, 2017, pp. 34-40.
[7] Mekki K., Bajic E., Chaxel F., Meyer F. A Comparative Study of LPWAN Technologies for Large-Scale IoT Deployment. ICT Express. Vol. 5, no. 1, 2019, pp. 1-7.
[8] Cotrim J. R. G., Kleinschmidt J. H. LoRaWAN Mesh Networks: A Review and Classification of Multihop Communication. Sensors. Vol. 20, no. 15, 2020.
[9] Lee H.-C., Ke K.-H. Monitoring of Large-Area IoT Sensors Using a LoRa Wireless Mesh Network System: Design and Evaluation. IEEE Transactions on Instrumentation and Measurement. Vol. 67, no. 9, 2018, pp. 2177-2187.
[10] Ebi C., Schaltegger F., Rüst A., Blumensaat F. Synchronous LoRa Mesh Network to Monitor Processes in Underground Infrastructure. IEEE Access. Vol. 7, 2019, pp. 57663-57677.
[11] Berto R., Napoletano P., Savi M. A LoRa-Based Mesh Network for Peer-to-Peer Long-Range Communication. Sensors. Vol. 21, no. 13, 2021.
[12] Douklias A. et al. A Field Communication System for Volunteer Urban Search and Rescue Teams Combining 802.11ax and LoRaWAN. Applied Sciences. Vol. 13, no. 10, 2023.
[13] Polonelli T., Brunelli D., Marzocchi A., Benini L. Slotted ALOHA on LoRaWAN - Design, Analysis, and Deployment. Sensors. Vol. 19, no. 4, 2019.
[14] Khadr M. H. et al. Jamming Resilient Multi-Channel Transmission for Cognitive Radio IoT-Based Medical Networks. Journal of Communications and Networks. Vol. 24, no. 6, 2022, pp. 666-678.
[15] Haykin S. Cognitive Radio: Brain-Empowered Wireless Communications. IEEE Journal on Selected Areas in Communications. Vol. 23, no. 2, 2005, pp. 201-220.
[16] Wang Q. et al. An Overview of Emergency Communication Networks. Remote Sensing. Vol. 15, no. 6, 2023.
[17] Höchst J. et al. LoRa-based Device-to-Device Smartphone Communication for Crisis Scenarios. In: ISCRAM 2020 Conference Proceedings. 2020, pp. 996-1011.